Biochemical and Biophysical Research Communications 427 (2012) 154–158

Contents lists available at SciVerse ScienceDirect

Biochemical and Biophysical Research Communications

journal homepage: www.elsevier.com/locate/ybbrc

Protein expression and isotopic enrichment based on induction of the Entner–Doudoroff pathway in *Escherichia coli*

Bosmat Refaeli, Amir Goldbourt *

School of Chemistry, Raymond and Beverly Sackler Faculty of Exact Sciences, Tel Aviv University, Ramat Aviv 69978, Tel Aviv, Israel

ARTICLE INFO

Article history:
Received 5 September 2012
Available online 17 September 2012

Keywords:
Entner–Doudoroff pathway
Protein expression
Nuclear magnetic resonance
Isotopic labeling
Sparse labeling
[1-^{13}C]-gluconate

ABSTRACT

The Entner–Doudoroff pathway is known to exist in many organisms including bacteria, archea and eukarya. Although the common route for carbon catabolism in *Escherichia coli* is the Embden–Meyerhof–Parnas pathway, it was shown that gluconate catabolism in *E. coli* occurs via the Entner–Doudoroff pathway. We demonstrate here that by supplying BL21(DE3) competent *E. coli* cells with gluconate in a minimal growth medium, protein expression can be induced. Nuclear magnetic resonance data of over-expressed ubiquitin show that by using [1-^{13}C]-gluconate as the only carbon source, and ^{15}N-enriched ammonium chloride, sparse isotopic enrichment in the form of a spin-pair carbonyl-amide backbone enrichment is obtained. The specific amino acid labeling pattern is analyzed and is shown to be compatible with Entner–Doudoroff metabolism. Isotopic enrichment serves as a key factor in the biophysical characterization of proteins by various methods including nuclear magnetic resonance, mass spectrometry, infrared spectroscopy and more. Therefore, the method presented here can be applied to study proteins by obtaining sparse enrichment schemes that are not based on the regular glycolytic pathway, or to study the Entner–Doudoroff metabolism during protein expression.

1. Introduction

The Entner–Doudoroff (ED) metabolic pathway has been discovered in *Pseudomonas saccharophila* in 1952 [1] and describes the initial steps of carbon catabolism in the cell. It was shown that when *Ps. saccharophila* is fed with glucose, which is radio-labeled at its C1 position, all the ^{14}C signals are recovered as $^{14}CO_2$ that originates from carboxyl-labeled pyruvate. This result differs from the common Embden–Meyerhof–Parnas (EMP) glycolitic pathway [2], the more common route for the breakdown of carbon, which predicts that C1 is converted to the methyl carbon in pyruvate. It was later discovered that the pathway exists in many other *Pseudomonas* species [3], in other organisms [4] and most importantly in *Escherichia coli* [5]. In particular, when *E. coli* cells are fed with gluconate as their sole carbon source, the ED pathway becomes the dominant route for carbon catabolism [6]. Detailed studies of the ED pathway have been performed in order to study its key enzymes demonstrating that the key factors are the missing phosphofructokinase and active 6-phosphogluconate dehydratase (EDD) and KDPG aldolase (EDA) [7,8].

Isotopic labeling of proteins and other macromolecules serves as a key factor in the biophysical characterization of their structure, function and dynamics. A variety of methods, including nuclear magnetic resonance, mass spectrometry, infrared spectroscopy and more, use isotopic enrichment in order to enhance sensitivity and resolution [9,10]. For example, over-expression [11] in *E. coli* using a minimal medium that is based on enriched isotopes is a common technique for producing proteins for NMR studies, enabling the characterization their structure and dynamics. Multi-dimensional NMR experiments are an essential tool in these studies [12,13] and require the use of NMR-active isotopes such as ^{2}H, ^{13}C and ^{15}N. Sparse isotopic enrichment of proteins also bears many advantages [14–19]; the elimination of the non-enriched carbons from the spectra results in better resolution allowing the study of larger proteins; relayed transfers are minimized enabling more accurate structure determinations; coupling of attached carbons is removed in many cases producing narrower lines in magic-angle spinning (MAS) NMR experiments and easier interpretation of relaxation data in solution NMR [20]. More specifically, the first protein structure determination by MAS NMR was facilitated by the use of 1,3-^{13}C and 2-^{13}C enriched glycerol media [21], a labeling scheme that was developed earlier for measuring thioredoxin dynamics by solution NMR [22]. Additional examples are the successful quantitative dynamics and binding studies of the 670 kDa 20S proteosome [23] by solution NMR using keto-acid labeling strategies [14] and the combined cryo-EM/solid-state NMR structure elucidation of the type III secretion system, a hollow needle-like protein filament of *E. coli*, using 1-^{13}C glucose and 2-^{13}C glucose as precursors for carbon [24]. The labeling

* Corresponding author. Fax: +972 3 6409293.
E-mail address: amirgo@post.tau.ac.il (A. Goldbourt).

0006-291X/$ - see front matter © 2012 Elsevier Inc. All rights reserved.
http://dx.doi.org/10.1016/j.bbrc.2012.09.031

patterns generated by these precursors, and by other carbon precursors [14,15,19,25,26], are all based on the EMP pathway, which is the main route for the breakdown of carbon in *E. coli*. There is therefore an increasing importance in creating diverse enrichment schemes that will enable the studies of proteins with larger complexity and molecular weight, for unfolded proteins, membrane proteins, and aggregated proteins, all examples of systems that produce highly congested NMR spectra. As opposed to protein overexpression, the production of bacteriophage viruses depends on the specific host that they infect. It was demonstrated that when the filamentous bacteriophage Pf1 is produced in its specific host, *Pseudomonas aeruginosa strain* K (PAK), carbon catabolism follows the Entner–Doudoroff (ED) pathway and not the EMP pathway. Therefore, when 1-^{13}C glucose (and $^{15}NH_4Cl$) was used as the sole carbon precursor for Pf1 growth, a ^{15}N–^{13}C' spin-pair backbone labeling scheme was obtained [27] rather than the enrichment of mainly aliphatic carbons [25,28]. However, up to now, it was not possible to use this pathway in general for every protein of choice, since it is not possible to over express proteins in this pathogenic strain.

Here we demonstrate that the ED pathway can be induced in *E. coli* strains suitable for protein expression, and therefore the sparse labeling schemes that arise are different from those produced following the EMP pathway [2], the common route for glycolysis, and follow the ED pathway. As an example, a spin-pair backbone labeling scheme is shown, in which many but not all carbonyl carbons are enriched to various degrees. Some sidechain methyl and carboxyl groups are fractionally labeled as well.

2. Materials and methods

A pET15-ubiquitin plasmid bearing a His-tag and kanamycin resistance (104 residues) has been transformed into Novagen *E. coli* BL21(DE3) competent cells grown on a typical LB-agar plate using normal procedures [11]. Reference unlabeled samples for testing induction were grown in a minimal medium containing gluconate and ammonium chloride using common protein expression techniques [11]. A [1-^{13}C]-gluconate labeled sample was obtained by growing a single colony in a starter LB medium. The preliminary culture was then transferred in a 1:100 ratio to a 1 L of M9 medium with unlabeled gluconate (5 g/L) and NH_4Cl (2 g/L). The unlabeled culture was pelleted at log phase, washed, and redissolved in similar concentrations of 1-^{13}C gluconate/$^{15}NH_4Cl$ enriched precursors within a minimal medium with a 1:4 volume ratio [29]. After 1 h the cells were induced with 0.8 mM IPTG, centrifuged, and lyzed using a microfluidizer. Purification was carried out on a Profinity IMAC Ni-charged resin (BIO-RAD) followed by dialysis against a 20 mM sodium-citrate buffer (pH 4.1, 10% D_2O). In all cases, pure protein yields per one liter of unlabeled starting media were 14–18 mg. Solution NMR experiments were performed on a Bruker DRX-500 MHz using a dual probe (1D experiment) and a TXI probe with a Z-gradient (HSQC and HNCO). For the HSQC experiment (acquired in 65 min.), 235/2048 points were acquired in t1/t2 for a total of 58/128 ms acquisition times. Data were linear predicted in the indirect dimension, apodized with a squared cosine and zero filled to 512 t1 points. For HNCO (17 h), 96/40/2048 points were acquired (17.5/11/128 ms) and processed with linear prediction in both indirect dimensions followed by cosine square apodization and zero filling to 512/256/2048 points. In both experiments 16 scans were acquired with a repetition rate of 1 s. The relative peak intensities, and therefore the relative enrichments (with respect to Val), were determined by taking both volume and peak height ratios (determined from Sparky [30]) of the HSQC and HNCO spectra, and then averaging over peaks with preceding carbonyls belonging to similar amino acids. A few peaks showed large deviations from the average, and were therefore dropped. [1-^{13}C]-gluconate precursor was obtained from Cambridge isotope laboratories with an enrichment level of 99.4%.

3. Results and discussion

The principal step in the ED pathway (Fig. 1) is the dehydrogenation of glucose-6 phosphate (G6P) to 6-phosphogluconate (6PG), replacing the conversion to fructose-1,6-bisphosphate (FBP) that normally occurs in the EMP pathway. This step results from the lack of the enzyme phosphofructokinase (*pfk*) in organisms in which the ED pathway is naturally occurring. In the EMP pathway, FBP is converted to pyruvate and gylceraldehyde 3-phosphate (G3P/GAP). However in the ED pathway, 6PG is converted to 2-keto-3-deoxy-6-phosphogluconate (KDPG) in a reaction catalyzed by 6-phosphogluconate dehydratase (EDD) and KDPG is converted to pyruvate and to G3P in a reaction catalyzed by KDPG aldolase (EDA). In both pathways, G3P goes through a series of reactions that generate precursors for the synthesis of serine, glycine and cystein (from 3PG, 3-phosphoglycerate) as well as phosphoenolpyruvate (PEP) that enters the pentose phosphate pathway (PPP) resulting in biosynthesis of aromatic amino acids and the TCA cycle generating oxaloacetate [2,31]. Although the final products of the two pathways are the same, i.e. pyruvate and G3P, the fate of the carbons of the precursor are different; while in EMP C-1 of glucose (marked ^{13}C in Fig. 1) occupies the methyl position in pyruvate, in the ED pathway it occupies the carbonyl carbon. The ED pathway is the preferred catabolic route in many *Pseudomonas* bacteria however, when *E. coli* is nurtured with gluconate, the formation of gluconokinase [6] is induced (and two additional enzymes of the ED pathway, EDD and EDA), leading to the production of 6PG, and therefore *E. coli* is forced to follow the ED pathway.

We have shown in the past that for the Pf1 filamentous bacteriophage [27], the host of which is *Ps. aeruginosa*, the naturally occurring ED pathway leads to carbonyl enrichment if the bacterial culture is fed with [1-^{13}C]-glucose. Consequently, line narrowing and spectral simplification were obtained in a multi-dimensional 3D NCC magic-angle spinning solid-state NMR experiment. The resulting spectra were used for the identification of the chemical shifts of the isotopically labeled carbonyl carbons belonging to the capsid of the intact virus. Furthermore, Kay et co. have shown [32,33] that by feeding *E. coli* directly with [1-^{13}C]- pyruvate, a carbonyl enrichment patterns is also obtained and can be used for measuring invisible and excited protein states using solution NMR.

In order to verify whether protein expression in a minimal medium containing gluconate follows the ED pathway, we transformed competent *E. coli* cells with a plasmid coding for ubiquitin. Cells were grown initially on unlabeled gluconate and ammonium chloride and the presence of over-expressed ubiquitin was then verified by SDS–PAGE (Supporting Fig. S1). Once expression was verified, a fresh cell culture was grown to log phase using the same unlabeled precursors and pelleted at log phase. These cells were then washed and resuspended in a minimal M9 medium containing [1-^{13}C]-gluconate and $^{15}NH_4Cl$ as the sole carbon and nitrogen sources, respectively, induced after 1 h and purified. We then performed NMR experiments in solution on the purified ubiquitin sample. The spectrum in Fig. 2, resulting from a ^{13}C single pulse experiment, shows that indeed the dominant signal comes from the carbonyl carbons, that the backbone Cα carbons are completely suppressed and that sidechains of distinct amino acids have also been labeled. Most of these aliphatic resonances have already been associated with the existence of labeled carbonate ions in the growth medium [27]; they result from the release of $^{13}CO_2$ during several processes such as the entry of pyruvate into the TCA cycle, the conversion of α-ketoisovalerate to leucine and the entry of 6PG

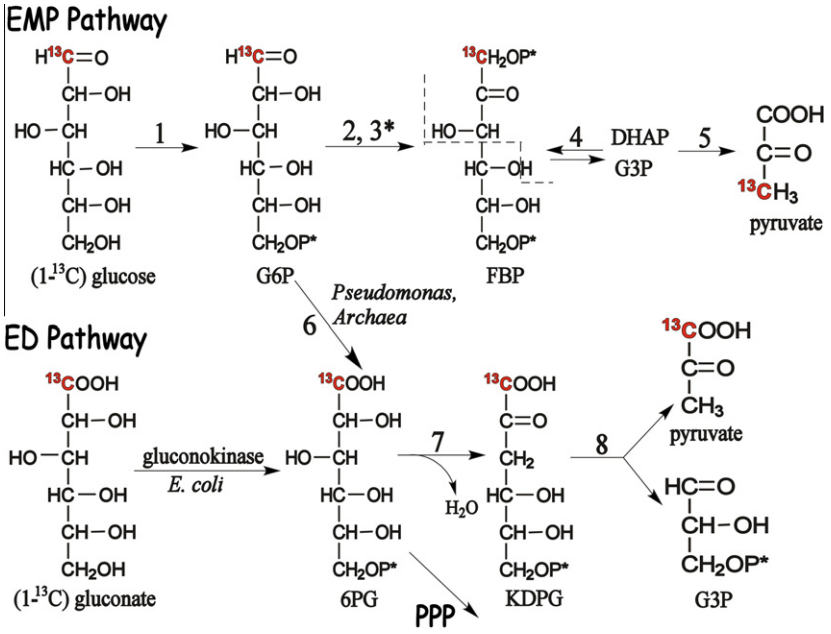

Fig. 1. The fate of a 1-^{13}C label in glucose and gluconate in the EMP and ED pathways. The enzymes catalyzing the reactions are indicated by their corresponding numbers. While *E. coli* will normally follow the EMP pathway, gluconate will induce the formation of gluconokinase as well as enzymes 7 and 8. *Pseudomonas* and some other bacteria follow the ED pathway stemming from glucose via enzyme 6. Acronyms are G6P, glucose-6-phosphate; FBP, fructose-1,6-bisphosphate; DHAP, dihydroxyacetone-phosphate; G3P, glyceraldehyde-3-phosphate; 6PG, 6-phosphogluconate; KDPG, 2-keto-3-deoxy-6-phosphogluconate. PPP indicates a transfer to the pentose phosphate pathway. The enzymes are: 1, glucokinase; 2, phosphoglucose isomerase; 3*, phosphofructokinase, the lack of this enzyme in *Pseudomonas* leads to the induction of the ED pathway; 4, fructose bisphosphate aldolase; 5 represents several different reactions; 6, G6P dehydrogenase; 7, 6-phosphogluconate dehydratase; 8, KDPG aldolase.

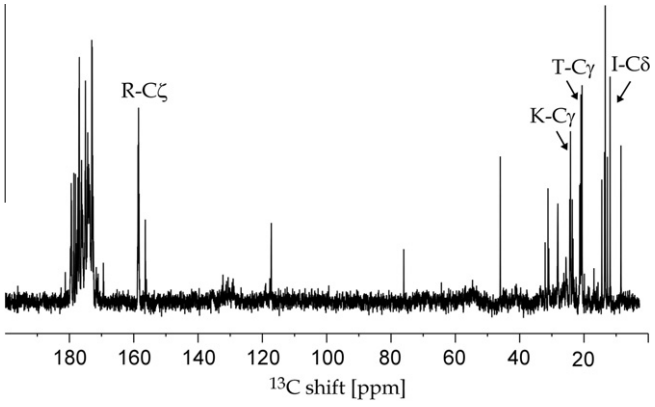

Fig. 2. The ^{13}C single-pulse solution NMR spectrum of [1-^{13}C]-gluconate labeled ubiquitin. Carbonyl enrichment and the lack of Cα are apparent. Sidechain signals from Ile-Cδ, Thr-Cγ, Lys-Cγ and Arg-Cζ are indicated. The experiment was acquired with an acquisition time of 0.6 s, 1550 scans, a relaxation time of 5 s and Waltz16 decoupling, and was processed with a line broadening of 3 Hz.

into the penthose phosphate pathway [2,31]. Of the sidechain carbons we assign, Ile-Cδ, Thr-Cγ, and Lys-Cγ are all products of 4-^{13}C oxaloacetate, which is an intermediate of the TCA cycle; Arg-Cζ stems from carbamoyl phosphate, a product of the urea cycle and the cellular pool of labeled bicarbonate [26,31] (see also Supplementary data).

According to the ED pathway, the highest level of carbonyl incorporation should be observed in the amino acids Val, Ala and Lys, however many other carbonyl carbons have been enriched as well. The identity of those carbons and their relative degrees of enrichment in this particular scheme, were obtained by comparing the 2D ^{1}H–^{15}N HSQC solution NMR spectrum of ubiquitin with data from a 3D HNCO experiment taken on the same sample. In HSQC, all amide groups are detected regardless of the carbon enrichment pattern. However, in HNCO a ^{15}N resonance of residue i will only appear in the spectrum if a neighboring C'_{i-1} is labeled, and its intensity will reduce with decreasing enrichment of this neighboring carbonyl. The overlay of the 2D HSQC with the H–N projection of the 3D HNCO spectrum is shown in Fig. 3. Despite some apparent overlap in the spectra due to the additional length of the his-tagged ubiquitin construct (104 residues), the resolution in the 3D spectrum was sufficient to identify nearly 90% of the resonances of the wild-type ubiquitin (the chemical shift were transferred from BioMagneticResonanceBank (bmrb) entry 15410 [35], where 70 of 76 ^{15}N and $^{13}C'$ resonances have been deposited). More important for demonstrating the enrichment pattern, all amino acid types existing in ubiquitin were unambiguously identified. Interestingly, most of the peaks appear in both spectra (carbonyl carbons belonging to 16 of the 18 amino acids in ubiquitin) however with significantly different intensities.

All the peaks that do not show up in the HNCO spectrum could be associated with a preceding Leu or His residues, and therefore these are the only residues not enriched at their C' positions. The lack of enrichment on leucine is a result of the loss of one labeled pyruvate carbonyl during the conversion of two pyruvate molecules to α-acetolactate (catalyzed by acetolactate synthase), which is a precursor for both valine and leucine, and the second labeled carbonyl upon the conversion of β-isopropylmalate to α-oxoisocaproate (catalyzed by β-isopropylmalate dehydrogenase). The carbonyl in leucine comes from acetyl-CoA when α-isopropylmalate is generated from α-oxoisovalerate (β-isopropylmalate synthase). Histidine biosynthesis starts with the conversion of carbonyl labeled 6PG to ribose-5-phosphate (R5P) during entrance to the pentose phosphate pathway, accompanied by the loss of the enriched carbon. Further conversion of R5P to 5-phophoribosyl-1-pyrophosphate starts a series of reactions that generate the unlabeled histidine. Sketches of the main pathways leading to the loss of labels are given in the Supplementary data.

Peaks from twelve different sequential amino acids pairs ($^{13}C_{i-1}$–$^{15}N_i$) representing different biosynthetic routes are indicated in the overlaid spectra of Fig. 3. The pairs associated with

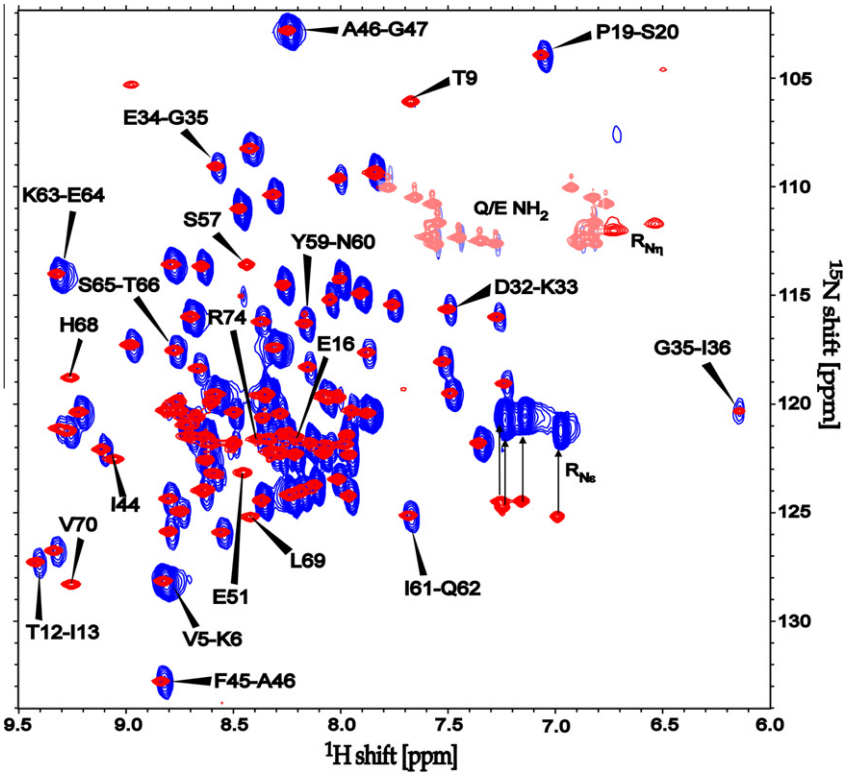

Fig. 3. A comparison of a 2D ^{1}H–^{15}N HSQC spectrum (red, narrow lines) with the ^{1}H–^{15}N (blue) projection of a 3D HNCO spectrum of a 1 mM his-tagged ubiquitin sample (over-expressed in the presence of [1-^{13}C]-gluconate and $^{15}NH_4Cl$). The amino acid *i*–*1*↔*i* pairs (from HNCO) were assigned based on the 70 resonances (from a total of 76 in wild-type ubiquitin) appearing in bmrb entry 15410 [34] and indicate the existence of a ^{13}C enriched carbonyl at residue *i*–*1*. Twelve representative pairs from HNCO are explicitly noted, out of overall 53 HNCO signals and 65 HSQC signals, which have been assigned. Backbone signals appearing only in the 2D HSQC spectrum are labeled according to amino acid *i*; they belong to the following pairs: L69–V70, L43–I44, L67–H68, L50–E51, L56–S57, L8–T9, L73–R74, H68–L69. All these signals indicate the lack of a carbonyl label on Leu and His residues. Resonances belonging to Arg-Nε have been folded differently in the 2D and 3D spectra but have similar shifts. Residues belonging to the sidechain amide groups of Asn and Gln are indicated by faint colors and in the HNCO spectrum they result from fractional labeling of the carbonyl sidechain carbon by oxaloacetate and α-ketoglutarate, respectively. (For interpretation of the references to colour in this figure legend, the reader is referred to the web version of this article.)

Val and Ala, V5–K6 and A46–G47 have the most intense signals and are both direct products of pyruvate. Comparison of the two pairs associated with Val (V5, V26) to those of Ala (A28, A46) shows that the enrichment of Ala is ~70% of Val, somewhat lower but in agreement with the observation made when 1-^{13}C pyruvate was used as a precursor for protein expression that is based on the EMP pathway [33]. Lys shows also relatively high degree of enrichment (54% of Val, the average of 6 signals; K63–E64 in Fig. 3) since its carbonyl stems from two sources; the incorporation of labeled pyruvate into β-aspartate-semialdehyde during its biosynthesis from aspartate [26,31] and through oxaloacetate, an intermediate of the TCA cycle. Additional products of the TCA cycle resulting directly from oxaloacetate are represented by T12–I13, D32–K33 and I61–Q62. They denote a very low C′ enrichment (between 10%–15% of Val) of Asp, Asn, Thr and Ile. The incorporation levels are low since upon entry to the TCA cycle pyruvate looses the carbonyl hence their enrichment is only a result of scrambling within the TCA cycle. The level of incorporation is lower than that reported for a 1-^{13}C pyruvate medium since the other source of oxaloacetate synthesis is PEP, which is largely unlabeled in this case as it is a product of G3P, the unlabeled part of the original gluconate precursor. Additional amino acids derived from the TCA cycle are Pro, Glu, Gln and Arg (15%–30%, represented by the signals of P19–S20 and E34–G35), all products of α-ketoglutarate. Finally, the largest difference from the EMP-based pyruvate enrichment scheme is in the accumulation of the enriched aromatic amino acids Tyr and Phe and the products of 3PG, Gly and Ser. The aromatic amino acids are direct products of the entry of unlabeled PEP into the biosynthetic route of their precursor, chorismate (e.g. F45–A46 and Y59–N60), hence the 4-fold reduction in the enrichment with respect to the 1-^{13}C pyruvate/$NaH^{13}CO_3$ medium. Ser and Gly (G35–I36 and S65–T66 in Fig. 3) are products of the unlabeled 3PG or the slow back conversion of enriched pyruvate to PEP and 3PG (also Cys, not present in the Ubq sequence). They are therefore enriched to low levels as well and only slightly over the enrichment of the aromatic amino acids. Indeed in the studies of the Pf1 virus [27], those four amino acids have not been observed at all, or gave very weak signals in the 3D experiment, probably due to the lower signal-to-noise of carbon-detected solid-state NMR experiment combined with their low enrichment.

In summary, the selective enrichment of carbonyls to various degrees (and the lower incorporation of aliphatic sidechain carbons) demonstrate that the BL21(DE3) competent *E. coli* strains are indeed amenable to protein over-expression under catabolism dominated by the ED pathway. The multi-dimensional solution NMR spectra of ubiquitin generated by this ^{15}N–$^{13}C'$ spin-pair backbone enrichment protocol are sufficiently resolved to allow site-specific identification of all amino acid types and the deduction of the labeling pattern. With the exception of Leu and His, all carbonyl carbons are enriched to some extent. Since only half of the precursor gluconate molecule generates actual isotope enrichment (similar to EMP-based enrichment schemes stemming from a singly labeled glucose), the degree of enrichment is between 5%–45%. These enrichment levels are approximately one-half of those obtained with a 1-^{13}C pyruvate-based medium for 12 amino acids, and much attenuated for amino acids stemming from the unlabeled part of the gluconate precursor (Ser, Gly, Phe, Tyr). Despite the relatively low enrichment, such labeling schemes

are useful for many applications in solution and solid state NMR [24,27,35,36]. Improvement in selectivity or in the extent of enrichment can be obtained by the incorporation of labeled or unlabeled bicarbonate, and other enrichment schemes can also potentially be designed by the incorporation of doubly labeled gluconate, and controlled by proper addition of unlabeled metabolites [19]. Another consequence of this study is the potential investigation of the metabolic pathways that occur in *E. coli* due to the gluconate uptake.

Acknowledgments

This work was supported by the Israel Science Foundation grant number 241/08. We thank Dr. Gali Prag from Tel Aviv University for providing us with the ubiquitin plasmid. We thank Limor Frish from Tel Aviv University for help with the NMR experiments.

Appendix A. Supplementary data

Supplementary data associated with this article can be found, in the online version, at http://dx.doi.org/10.1016/j.bbrc.2012.09.031.

References

[1] N. Entner, M. Doudoroff, Glucose and gluconic acid oxidation of pseudomonas saccharophila, J. Biol. Chem. 196 (1952) 853–862.
[2] G. Gottschalk, Bacterial Metabolism, Springer, New York, 1985.
[3] I.J. Stern, C.H. Wang, C.M. Gilmour, Comparative catabolism of carbohydrates in pseudomonas species, J. Bacteriol. 79 (1960) 601–611.
[4] T. Fuhrer, E. Fischer, U. Sauer, Experimental identification and quantification of glucose metabolism in seven bacterial species, J. Bacteriol. 187 (2005) 1581–1590.
[5] N. Peekhaus, T. Conway, What's for dinner?: Entner–Doudoroff metabolism in Escherichia coli, J. Bacteriol. 180 (1998) 3495–3502.
[6] R.C. Eisenberg, W.J. Dobrogosz, Gluconate metabolism in Escherichia coli, J. Bacteriol. 93 (1967) 941–949.
[7] T. Conway, The Entner–Doudoroff pathway: history, physiology and molecular biology, FEMS Microbiol. Lett. 103 (1992) 1–27.
[8] T.G. Lessie, P.V. Phibbs, Alternative pathways of carbohydrate utilization in pseudomonads, Annu. Rev. Microbiol. 38 (1984) 359–388.
[9] E. Roth, Critical evaluation of the use and analysis of stable isotopes, Pure Appl. Chem. 69 (1997) 1753–1828.
[10] P.I. Haris, G.T. Robillard, A.A. Van Dijk, D. Chapman, Potential of carbon-13 and nitrogen-15 labeling for studying protein-protein interactions using fourier-transform infrared spectroscopy, Biochemistry 31 (1992) 6279–6284.
[11] J. Sambrook, D.W. Russell, Molecular Cloning: A Laboratory Manual, Cold Spring Harbor Laboratory Press, 2001.
[12] J. Jeener, Ampere International Summer School, Basko Polje, Yugoslavia, 1971.
[13] L. Muller, A. Kumar, R.R. Ernst, Two-dimensional carbon-13 NMR spectroscopy, J. Chem. Phys. 63 (1975) 5490–5491.
[14] V. Tugarinov, V. Kanelis, L.E. Kay, Isotope labeling strategies for the study of high-molecular-weight proteins by solution NMR spectroscopy, Nat. Protoc. 1 (2006) 749–754.
[15] S.-y. Ohki, M. Kainosho, Stable isotope labeling methods for protein NMR spectroscopy, Prog. Nucl. Magn. Reson. Spectrosc. 53 (2008) 208–226.
[16] D. Neri, T. Szyperski, G. Otting, H. Senn, K. Wuthrich, Stereospecific nuclear magnetic resonance assignments of the methyl groups of valine and leucine in the DNA-binding domain of the 434 repressor by biosynthetically directed fractional 13C labeling, Biochemistry 28 (1989) 7510–7516.
[17] P. Lundstrom, P. Vallurupalli, D.F. Hansen, L.E. Kay, Isotope labeling methods for studies of excited protein states by relaxation dispersion NMR spectroscopy, Nat. Protoc. 4 (2009) 1641–1648.
[18] L.Y. Lian, D.A. Middleton, Labelling approaches for protein structural studies by solution-state and solid-state NMR, Prog. Nucl. Magn. Reson. Spectrosc. 39 (2001) 171–190.
[19] P. Gans, O. Hamelin, R. Sounier, I. Ayala, M.A. Durá, C.D. Amero, M. Noirclerc-Savoye, B. Franzetti, M.J. Plevin, J. Boisbouvier, Stereospecific isotopic labeling of methyl groups for NMR spectroscopic studies of high-molecular-weight proteins, Angew. Chem. Int. Ed. 49 (2010) 1958–1962.
[20] N.K. Goto, L.E. Kay, New developments in isotope labeling strategies for protein solution NMR spectroscopy, Curr. Opin. Struct. Biol. 10 (2000) 585–592.
[21] F. Castellani, B. van Rossum, A. Diehl, M. Schubert, K. Rehbein, H. Oschkinat, Structure of a protein determined by solid-state magic-angle-spinning NMR spectroscopy, Nature 420 (2002) 98–102.
[22] D.M. LeMaster, D.M. Kushlan, Dynamical mapping of E. coli thioredoxin via 13C NMR relaxation analysis, J. Am. Chem. Soc. 118 (1996) 9255–9264.
[23] R. Sprangers, L.E. Kay, Quantitative dynamics and binding studies of the 20S proteasome by NMR, Nature 445 (2007) 618–622.
[24] A. Loquet, N.G. Sgourakis, R. Gupta, K. Giller, D. Riedel, C. Goosmann, C. Griesinger, M. Kolbe, D. Baker, S. Becker, A. Lange, Atomic model of the type III secretion system needle, Nature 486 (2012) 276–279.
[25] P. Lundström, K. Teilum, T. Carstensen, I. Bezsonova, S. Wiesner, D. Hansen, T. Religa, M. Akke, L. Kay, Fractional ^{13}C enrichment of isolated carbons using [1-^{13}C]- or [2-^{13}C]-glucose facilitates the accurate measurement of dynamics at backbone C^{α}; and side-chain methyl positions in proteins, J. Biomol. NMR 38 (2007) 199–212.
[26] C.G. Hoogstraten, J.E. Johnson, Metabolic labeling: taking advantage of bacterial pathways to prepare spectroscopically useful isotope patterns in proteins and nucleic acids, Concepts in Magnetic Resonance Part A 32A (2008) 34–55.
[27] A. Goldbourt, L.A. Day, A.E. McDermott, Assignment of congested NMR spectra: carbonyl backbone enrichment via the Entner–Doudoroff pathway, J. Magn. Reson. 189 (2007) 157–165.
[28] M. Hong, Determination of multiple phi-torsion angles in proteins by selective and extensive C-13 labeling and two-dimensional solid-state NMR, J. Magn. Reson. 139 (1999) 389–401.
[29] J. Marley, M. Lu, C. Bracken, A method for efficient isotopic labeling of recombinant proteins, J. Biomol. NMR 20 (2001) 71–75.
[30] T.D. Goddard, D.G. Kneller, SPARKY 3.1.1, University of California, San Francisco, CA.
[31] D. Voet, J.G. Voet, Biochemistry, third ed., Wiley, New York, 2004.
[32] D.F. Hansen, P. Vallurupalli, P. Lundström, P. Neudecker, L.E. Kay, Probing chemical shifts of invisible states of proteins with relaxation dispersion NMR spectroscopy: how well can we do?, J Am. Chem. Soc. 130 (2008) 2667–2675.
[33] P. Lundström, D. Hansen, L. Kay, Measurement of carbonyl chemical shifts of excited protein states by relaxation dispersion NMR spectroscopy: comparison between uniformly and selectively ^{13}C labeled samples, J. Biomol. NMR 42 (2008) 35–47.
[34] V.A. Jaravine, A.V. Zhuravleva, P. Permi, I. Ibraghimov, V.Y. Orekhov, Hyperdimensional NMR spectroscopy with nonlinear sampling, J. Am. Chem. Soc. 130 (2008) 3927–3936.
[35] N. Nishida, F. Motojima, M. Idota, H. Fujikawa, M. Yoshida, I. Shimada, K. Kato, Probing dynamics and conformational change of the GroEL-GroES complex by 13C NMR spectroscopy, J. Biochem. 140 (2006) 591–598.
[36] K. Kato, C. Sautès-Fridman, W. Yamada, K. Kobayashi, S. Uchiyama, H. Kim, J. Enokizono, A. Galinha, Y. Kobayashi, W.H. Fridman, Y. Arata, I. Shimada, Structural basis of the interaction between IgG and fcγ receptors, J. Mol. Biol. 295 (2000) 213–224.